

See discussions, stats, and author profiles for this publication at: <https://www.researchgate.net/publication/231695951>

New Ladder-Type Poly(p-phenylene)s Containing Fluorene Unit Exhibiting High Efficient Electroluminescence

ARTICLE *in* MACROMOLECULES · DECEMBER 2003

Impact Factor: 5.8 · DOI: 10.1021/ma034929q

CITATIONS

55

READS

11

7 AUTHORS, INCLUDING:



Song Qiu

Chinese Academy of Sciences

20 PUBLICATIONS 383 CITATIONS

SEE PROFILE



Ping Lu

Zhejiang University

334 PUBLICATIONS 6,868 CITATIONS

SEE PROFILE



Yuguang Ma

Chinese Academy of Sciences

310 PUBLICATIONS 6,280 CITATIONS

SEE PROFILE

New Ladder-Type Poly(*p*-phenylene)s Containing Fluorene Unit Exhibiting High Efficient Electroluminescence

Song Qiu, Ping Lu, Xiao Liu, Fangzhong Shen, Linlin Liu, Yuguang Ma,* and Jiacong Shen

Key Lab of Supramolecular Structure and Materials, Jilin University, Changchun 130023, P. R. China

Received July 3, 2003; Revised Manuscript Received August 28, 2003

ABSTRACT: A type of soluble and thermally stable ladder-type poly(*p*-phenylene) (LPF) with fluorene units in polymer backbone has been synthesized by Suzuki coupling and Friedel–Crafts ring-closing reaction. The full characterization of structures and properties as well as the performances of electroluminescence devices of the new ladder polymers are presented. LPFs show the well-defined structures, high molecular weights, excellent thermal stability, and good solubility in common organic solvents. The high-efficiency emission and absence of low-energy emission band in photoluminescence spectra are observed from LPFs both in the solution and in the solid film. Furthermore, the single layer light-emitting device using LPFs as the active layer shows very stable blue-green emission with maximum luminescence of 5400 cd/m² and maximum luminance efficiency of 0.66 cd/A. The extraordinary low concentration of keto defects in LPFs may be corresponding to the improvement in optical and device properties. The attractive properties exhibited by new ladder-type poly(*p*-phenylene)s establish them as good candidates for active layers in light-emitting devices.

Introduction

In the past few decades, conjugated polymers have attracted broad interest due to their potential application to full color flat panel displays.¹ Among these conjugated polymers, ladder-type poly(*p*-phenylene) (LPPP) and its derivatives are an important class of polymers materials served as active layer of light-emitting diodes (LEDs),² energy-transfer host material,³ and important model compound in photophysical research fields.⁴ In 1991, for the first time, Scherf and Müllen showed that structural regular LPPP (Chart 1a) can be obtained by intramolecular Friedel–Crafts ring-closing reaction of a designed soluble poly(*p*-phenylene).⁵ The original LPPP showed an unstructured broad emission from 460 to 600 nm in the solid state compared to its sharp fluorescence emission around 460 nm in solution. The low-energy emission band of LPPP contributed to the formation of the excimer owing to interchain interactions and π – π stacking interaction between the planar conjugated segments.⁶ Consequently, the distinct reduction of the low-energy emission band in the LPPP derivatives with slight structure variations such as MeLPPP (introduction of a methyl group at the methylene bridge) (Chart 1b) was obtained through introduction of spatial hindrance to inhibit the aggregation of planar conjugated polymers.⁷ Within the past 5 or 6 years MeLPPP has been intensively tested for many potential applications.⁸

However, recently Scherf et al. provided more powerful evidence indicating that the low-energy emission bands are due to keto defect sites in the polymer backbone, especially for the polyfluorene (PF) derivatives with methylene-bridged hydrogen substituents.⁹ It is reasonable that the defects in very low concentration (even no indication in the general analysis method, ca. IR and NMR) play a more important role for

photophysical properties of conjugated polymers because the excited energy migration along conjugated polymer chains and a transfer to defects are more efficient, especially in the solid state due to an additional interchain energy migration process. These results let us reconsider the possible defects in LPPP and search the possible route to depress the defect sites in LPPP. To look back at each step in the synthesis of LPPP, the incomplete reaction of keto groups in the reduction process and incomplete cyclization in the final Friedel–Crafts ring-closing reaction may induce the keto survivors. Thus, a careful study on both reactions is strongly required.

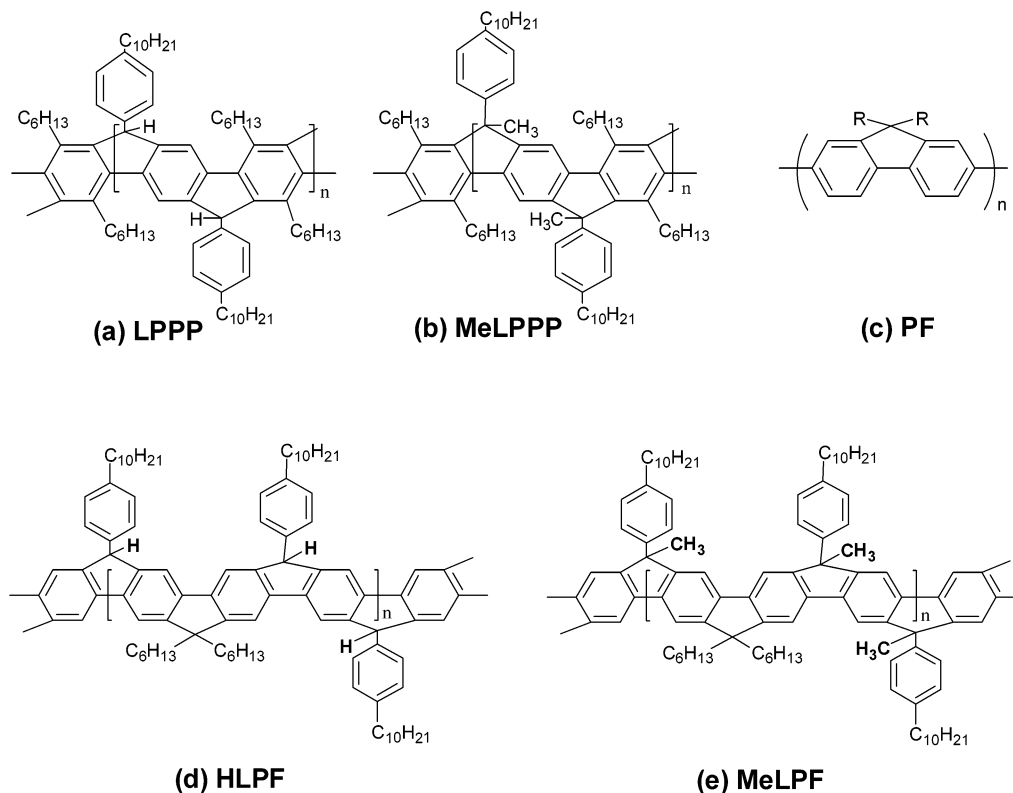
In this paper, we introduce a type of LPPP derivative (LPF, as shown in Chart 1d,e). Identical LPPP derivatives have been prepared by Forster (Scherf group) in 2000,¹⁰ but the detailed characteristics of polymer structure and measurement in physical properties, e.g., electroluminescence, are not studied. Different from LPPPs that were built from the phenylene units, the LPFs were obtained by the fluorene monomer as one of the initial building blocks. Since fluorene units are rigidly bridged and they occupy half of the skeleton in the precursor polymer before ring-closing reaction, this change can partially reduce the probability of the formation of defects originating from incomplete cyclization. The resultant LPFs exhibit distinct improvement in color purity, spectral stability, and the performance of LED devices. On the other hand, the incorporated fluorene units in LPFs backbone also provide the opportunity to modify the polymer properties by changing the substitutes at the active C-9 position of fluorene rings, as has been extensively used for the modification of fluorene-based conjugated polymers.¹¹

Results and Discussion

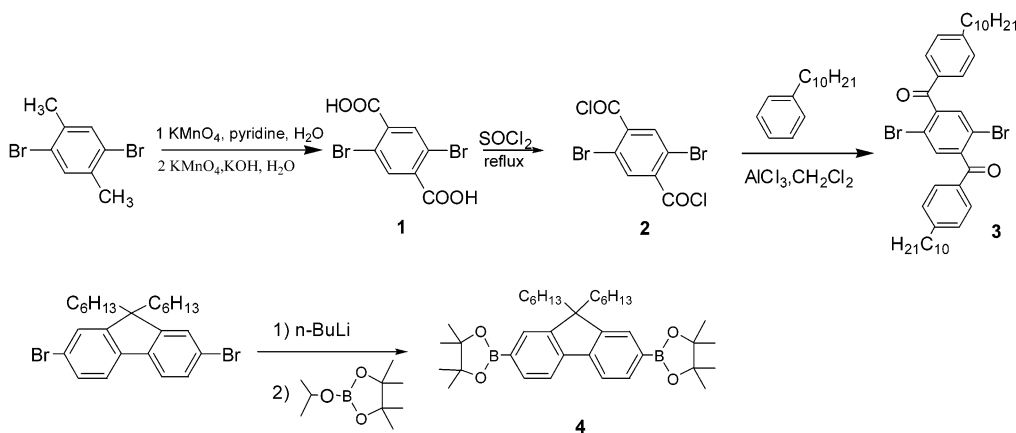
Synthesis and Characterization. Scheme 1 shows the synthetic routes to the monomers for LPFs. 1,4-Dibromo-2,5-benzenedicarboxylic acid (**1**) was synthe-

* Corresponding author: Fax +86-431-8980729, e-mail ygma@jlu.edu.cn.

Chart 1



Scheme 1. Synthetic Route to the Monomers, Reagents, and Conditions



sized via a two-step oxidation of 1,4-dibromo-*p*-xylene.¹² **1** was then converted to the 2,5-dibromoterephthaloyl dichloride (**2**) by treatment with thionyl chloride. To obtain 2',5'-dibromo-4-decyl-4'-(4-decylbenzoyl)benzophenone (**3**), the reaction of **2** with decylbenzene via Friedel–Crafts acylation in CH_2Cl_2 according to the literature was unsuccessful; however, in benzene solvent, **3** was obtained with a satisfactory yield of 72.3%. The copolymerized monomer 2,7-bis(4,4,5,5-tetramethyl-1,3,2-dioxaborolan-2-yl)-9,9-dihexylfluorene (**4**) was prepared using the well-known route.¹³

Scheme 2 shows the preparation of novel ladder poly(*p*-phenylene) with the well-known process.^{5,7} For the first step, the alternating copolymer **P1** can be prepared from a Suzuki coupling reaction between **3** and **4** using $(\text{PPh}_3)_4\text{Pd}(0)$ as catalyst in a mixture of toluene and 2 M K_2CO_3 aqueous solution for 2 days. For the second step, there exist two routes. One is the keto group alkylated with methyllithium to give **P2a**, and the other

is the keto group reduced with lithium aluminum hydride to give **P2b**. To obtain good quality LPPFs, the remaining keto groups must be reduced completely in this step, so the reducing agents methyllithium and lithium aluminum hydride are need largely excessive to ensure complete reduction of keto groups. For the last step, the final products, MeLPPF and HLPF, were obtained by the ring-closure reaction of **P2a** (**P2b**) with boron trifluoride etherate via a polymer-analogous intramolecular Friedel–Crafts alkylation. The polymers are yellow-green powder after repeated precipitation with CHCl_3 /methanol and are readily dissolved in common organic solvents such as chloroform, dichloromethane, tetrahydrofuran, toluene, and xylene.

The number-average molecular weights (M_n) and the weight-average molecular weights (M_w) of the polymers were measured by gel permeation chromatography (GPC) using polystyrene as a standard (Table 1). The M_n of MeLPPF is 22 000, corresponding to about 70

Scheme 2. Synthetic Route to MeLPF and HLPF

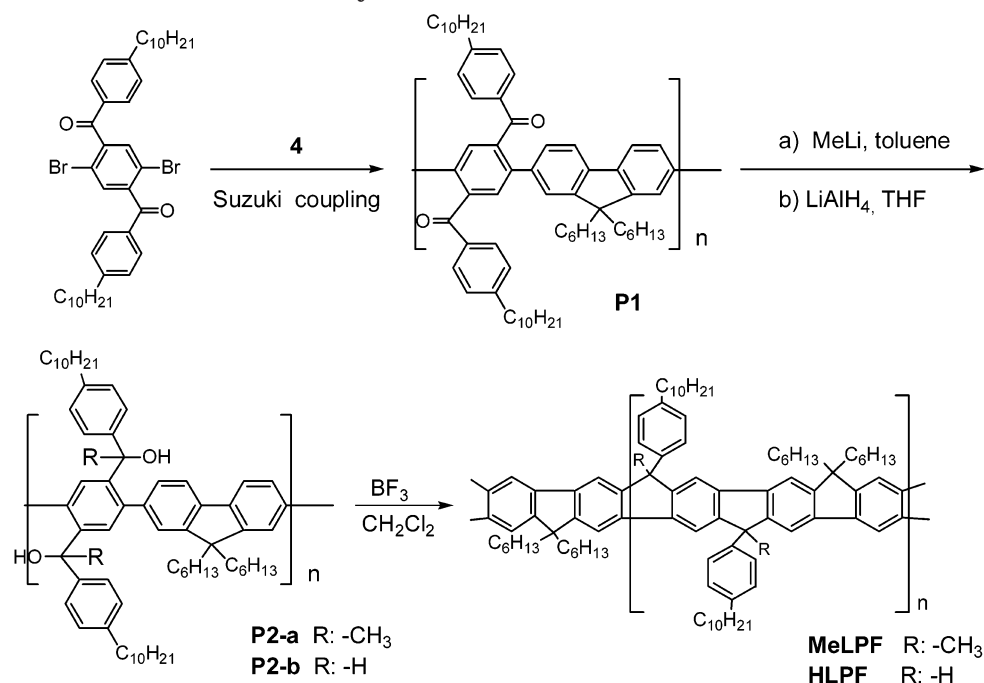


Table 1. Molecular Weight and the Thermogravimetric Analysis Data of MeLPF and HLPF

polymer	M_n	M_w	PD	T_d (°C)
MeLPF	22 307	42 864	1.92	358.3
HLPF	16 359	27 044	1.65	400.9

benzene rings (25 repeated units) in the backbone, which is a relatively high value in polymers synthesized using the Suzuki coupling reaction.

The chemical structures of LPFs were fully characterized by ^1H NMR, ^{13}C NMR, FT-IR, and elemental analysis. ^1H NMR and ^{13}C NMR spectra of polymers are consistent with the structure of the target polymers. Figure 1 shows the ^1H NMR spectrum of MeLPF. All proton and integral areas of the peak can match the polymer structure. The ^1H NMR spectrum of HLPF is similar to that of MeLPF; only an excessive signal appeared around 5.07 ppm which is ascribed to the proton in methylene bridge. The remaining $-\text{Ar}-\text{CHOH}-\text{Ar}-$ and keto groups were not detected in NMR spectra. In IR spectra of LPFs (Figure 2) the keto or hydroxyl groups in 1700 or 2500 cm^{-1} were not observed. From above the incomplete ring-closure reaction or defects were not found in LPFs.

MeLPF and HLPF exhibit good thermal stability measured by thermogravimetric analysis (TGA) under a nitrogen atmosphere. The polymers have onset degradation temperatures (T_d) above 358.3 and 400.9 °C, respectively. No weight loss is observed at lower temperatures. The phase transitions of the polymers were determined by differential scanning calorimetry (DSC) in a nitrogen atmosphere at a heating rate of 5 K/min, but we observed neither glass transition process (T_g) nor other thermal process (such as liquid-crystal phase) from 20 to 300 °C for MeLPF and HLPF.

Spectroscopic Properties. As shown in Figure 3, the UV-vis absorption and photoluminescence (PL) spectra of **P1** and **P2a** in THF solution present an enormous difference. The maximum absorption peak of **P1** was at 362 nm, while **P2a** and **P2b** are distinctly shifted toward high energy. The absorption band of **P1**

in the low-energy range can be explained by the interaction between the $n-\pi^*$ orbital of the keto substituents and the $\pi-\pi^*$ orbital of the conjugated backbone, and such interaction was absent in its reduced products **P2a** and **P2b**, resulting in an increase in absorption energy. An unstructured broad peak centered at ca. 500 nm was observed from the PL spectrum of **P1** solution, which is ascribed to keto substituents, while a pure-blue emission peaking at 410 nm and never the 500 nm peak was observed from **P2a** and **P2b** solution, suggesting the complete reduction of the keto group to hydroxyl.

Figure 4 shows the UV-vis absorption and PL spectra in solution and film of MeLPF and HLPF. The absorption spectra of LPFs display a steep absorption edge and a well-resolved vibrational energy band which indicates the character of a rigid, planar, one-dimensional π -system. The maximum absorption of MeLPF is red-shifted by 140 nm (0.74 eV) when compared with **P2a**. The PL spectra of LPFs in dilute solution presented three emission bands peaking around 460, 490, and 520 nm, which are mirror-plane symmetrical with the absorption spectra and are assigned as transition from the first excited-state S_1 to the ground-state S_0 with varied vibrational levels. At the same time, a very small Stokes shift less than 4 nm (140 cm^{-1}) is observed, and the magnitude of the Stokes shift and well-resolved vibrational energy band in electronic spectra can be interpreted as a consequence of the geometrically constrained rigid π -electron system, which permits no major geometric change in the transition from the ground state to the excited state. The PL efficiency (Φ_{PL}) of the polymers in chloroform was measured compared to quinine sulfate (ca. 2×10^{-5} M, assuming Φ_{PL} of 0.546 at 365 nm excitation in 1 N H_2SO_4)¹⁴ as standard. MeLPF and HLPF exhibited very high PL efficiencies in chloroform in the range of 72–83% (Table 2), corresponding to few routes existing for nonradiative deactivation.

The PL spectra in solid state of MeLPF (HLPF) are almost identical with that in dilute solution. The slight increase in relative intensity of 500–600 nm emission

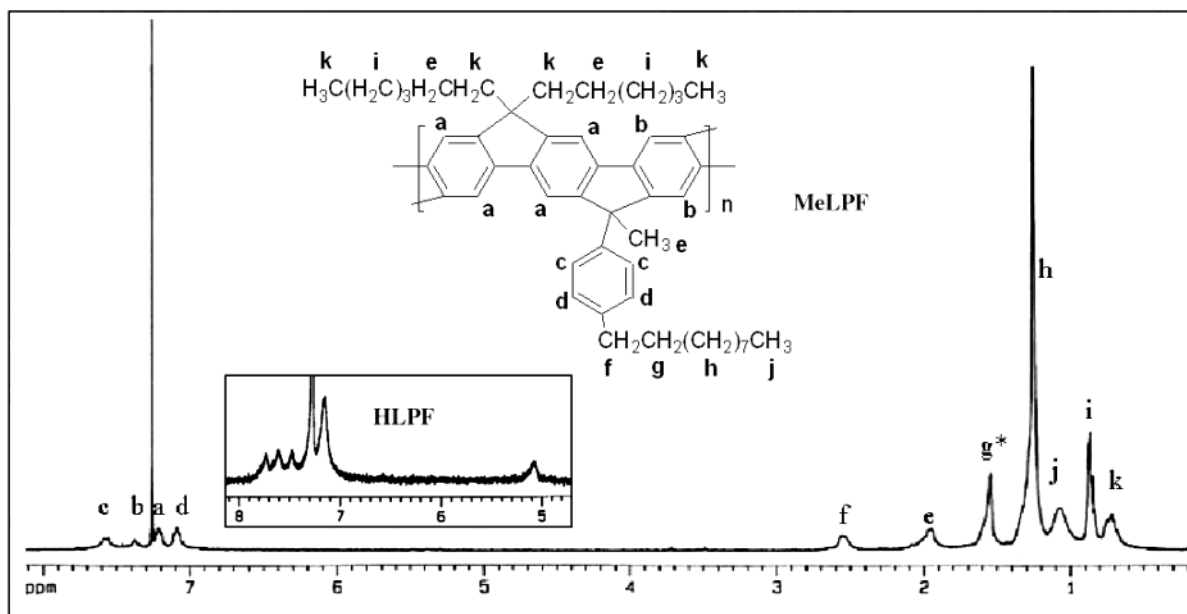


Figure 1. ^1H NMR spectra of MeLPF and HLPF in CDCl_3 . g^* contain the proton peak of water.

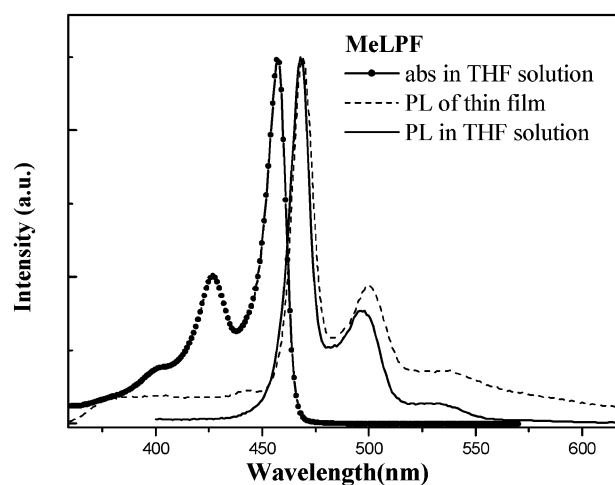
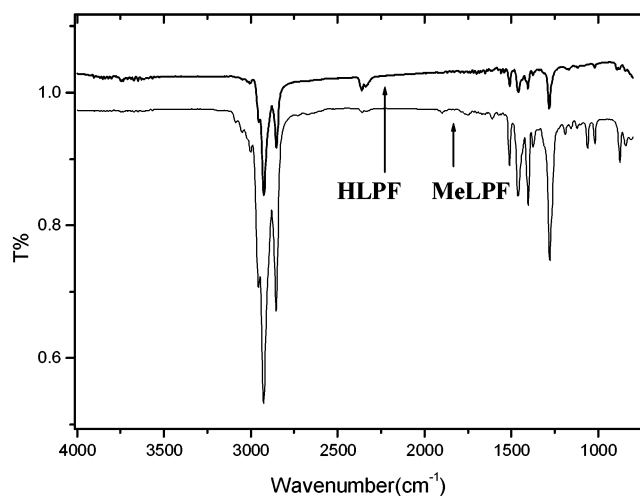


Figure 2. FT-IR spectra of MeLPF and HLPF.

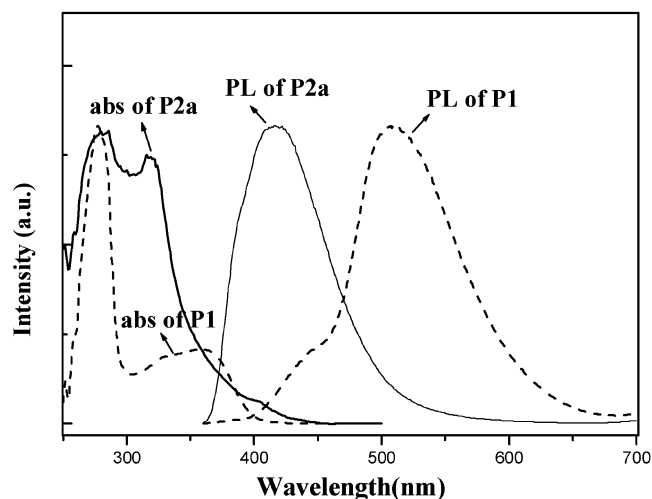


Figure 3. UV-vis absorption and PL spectra of **P1** and **P2** in THF solution.

in solid films may be ascribed to the stronger self-absorption effects than that in solution. Recently, on-chain chemical defects have been identified as one

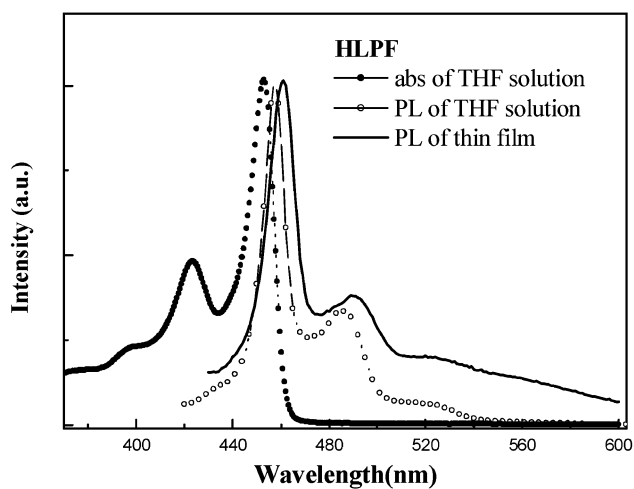


Figure 4. Absorption and PL spectra of MeLPF and HLPF in dilute THF solution and spin-coating thin film.

source of the low-energy emission in PF and LPPP, especially in PF derivatives with methylene-bridged hydrogen substituents.^{9,15} Generally, the low-energy emission from defects was enhanced in the film compared to corresponding solution because of the inter-

Table 2. Spectral Properties of Precursors and LPFs

polymer	abs (in THF) λ_{\max} (nm)	PL (in THF) ^a λ_{\max} (nm)	PL of film ^a λ_{\max} (nm)	PL efficiency in CHCl ₃ (Φ_{PL}) ^b (%)	E_g^c (eV)	EL λ_{\max} (nm)
P1	362	500	508		3.23	
P2a	318	405	415		3.15	
P2b	322	403	413		3.15	
HLPF ^d	(425) 455	459 (486)	460 (490)	74	2.70	460 (490)
MeLPF	(428) 459	464 (494)	464 (496)	83	2.68	464 (494)

^a Excited at 360 nm. ^b Calculated by the relative method.¹⁴ ^c Estimated from the onset wavelength of the optical absorption. ^d Peaks that appear as shoulders or weak bands shown in parentheses.

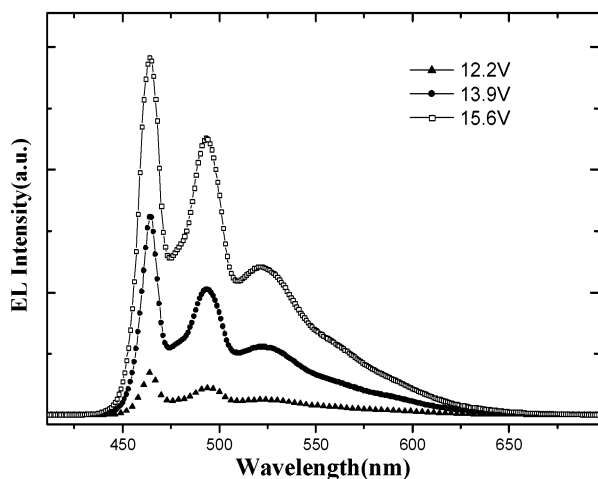


Figure 5. EL spectra of MeLPF (ITO/PEDOT/MeLPF/Ba/Ag) at different voltages.

chain migration of excited energy in film state which increased the probability of excited energy transfer to defects. However, in the PL spectra of LPFs in solid film, even HLPF which has hydrogen substituents at bridged methylene, the low-energy band is very low. The spectra are very stable even after annealing process at 180 °C for 12 h in a nitrogen atmosphere. From these results, no evidence indicates there is any keto defect in LPFs, which is agreement with the conclusions by general structural analysis, *ca.* IR and NMR. Sometimes we used the LPFs solution which was deposited for several weeks to cast film, and a new low-energy band around 540–560 nm can be observed in the PL spectra of the film; such a low-energy band is found to disappear when the film samples remained at room temperature for a few hours. Since the low-energy emission from keto defects of polymers cannot disappear, we thought the low-energy band was mostly ascribed to an interchain aggregate states between the planar polymer backbones^{6,16} and that aggregate state was not stable in film state even at room temperature. We will continue the photophysical study in following work.

Device Characteristics. The single-layer polymer light-emitting diodes (PLEDs) with the configuration of ITO/PEDOT:PSS/MeLPF/Ba/Ag were fabricated to investigate the electroluminescent properties of the LPFs. As shown in Figure 5, the EL spectra of MeLPF show a peak wavelength around 464 nm and a shoulder around 494 and 524 nm, which are similar to the PL spectra of the corresponding polymer film. The shape of spectra is very stable in different voltage. Figure 6 shows the current–brightness–voltage curves and the current density dependence of luminance efficiency for the device of ITO/PEDOT:PSS/MeLPF/Ba/Ag. With an increasing of forward bias voltage, the current and brightness in the devices increases. Light emitting is observed with turn-on voltage ranged from 7 to 12 V and the

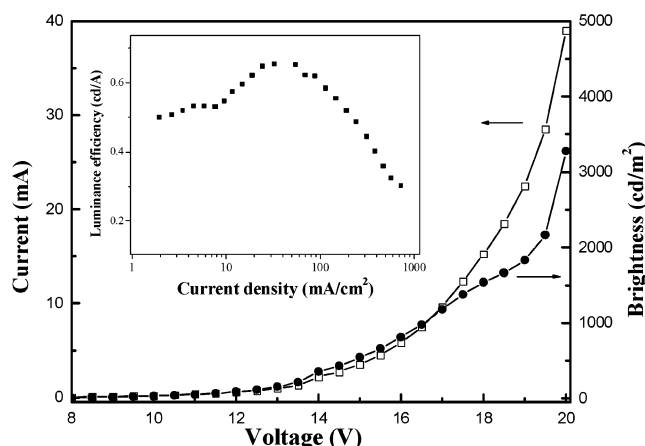


Figure 6. Current–brightness–voltage characteristics of the device (ITO/PEDOT/MeLPF/Ba/Ag). Inset: dependence of the luminance efficiency on the drive current density for the device.

maximum brightness up to 5600 cd/m² in the best device. The luminance efficiency first increases and then decreases with increasing current density; the maximum luminance efficiency of 0.66 cd/A is achieved at a current density of 33 mA/cm and a brightness of 289 cd/m². Further improvement in device efficiency and brightness can be obtained by adjusting device structure and electrode metals with more efficient injection and balanced transport of both charge carriers. The HLPF devices also show the EL spectra similar to the PL spectra of HLPF film and keep stable at different voltages with a lower luminance efficiency of 0.1 cd/A. These results are obviously different from the PL and EL spectra of the LPPP (Chart 1a) which emits an unstructured broad band from 460 to 600 nm.^{2,3,5}

From above, the low-energy emission band from the aggregation of planar polymers or keto defect sites cannot exert an effective influence to both PL and EL spectra of LPFs. The improvement in optical and device properties can correspond to the extraordinary low concentration of defects in LPFs. The stable spectral properties and the enhanced performances of devices indicated that the LPFs can be a useful material for light-emitting devices.

Conclusion

We prepared a type of soluble, thermally stable ladder-type poly(*p*-phenylene) with fluorene units in the polymer backbone by Suzuki coupling and presented full characterization of their structure and properties as well as electroluminescence performances. The polymers have high molecular weights, low defect in backbone, excellent thermal stability, good solubility in common organic solvents, and high PL efficiencies. Light-emitting devices using LPFs as the active layer show very stable blue-green emission. Furthermore, MeLPF de-

vices show a maximum luminescence of 5400 cd/m² and maximum luminance efficiency of 0.66 cd/A. The low-energy emission band from the aggregation of planar polymers or keto defect sites cannot exert an effective influence on both PL and EL spectra of LPFs. These attractive properties established the LPFs as widely useful materials for polymer-based optical and electrooptical applications.

Experimental Section

Measurement. ¹H and ¹³C NMR spectra were recorded on a Bruker AVANCZ 500 MHz spectrometer with chloroform-*d* as solvents and tetramethylsilane (TMS) as the internal standard. FT-IR spectra were recorded on a Bruker IFS66VFT-IR spectrometer in the 800–4000 cm⁻¹ regions by casting the solution of polymers on CaF substrate. UV-vis and fluorescence spectra were obtained on a Shimadzu UV-3100 spectrophotometer and a Shimadzu RF-5301PC spectrophotometer, respectively. Thermogravimetric analysis (TGA) was conducted on a Perkin-Elmer thermal analysis system under a heating rate of 20 K/min and a nitrogen flow rate of 80 mL/min. Differential scanning calorimetry (DSC) was also run on a Perkin-Elmer thermal analysis system. Elemental analysis was performed on a Flash EA 1112, CHNSO instrument. Number-average and weight-average molecular weights of polymer products were determined by gel permeation chromatography (GPC) with an HPLC Waters 510 using a series of monodisperse polystyrene as standards in THF (HPLC grade) at 308 K.

LED Device Fabrication and Characterization. PLED devices were fabricated on glass substrates coated with ITO. The substrate was cleaned by a general procedure, which included sonication in detergent followed by repeated rinsing in deionized water, acetone, and ethanol and, prior to use, placed in boiling H₂O₂ for 5 min. The conducting polymer dispersion of poly(3,4-ethylenedioxythiophene) doped with poly(styrenesulfonic acid) (PEDOT:PSS) was obtained from Bayer Corp. The hole injection layer of PEDOT:PSS was prepared from a water dispersion with a thickness of 50 nm and baked at 170 °C for 20 min under a N₂ atmosphere. The emitting layer of the polymer was spin-coated from an oxygen-free toluene solution onto the hole injection layer with a thickness of 100 nm. Finally, the Ba and Ag cathode was vacuum-deposited onto the polymer layers at a pressure below 5 × 10⁻⁶ Torr. The emitting areas of the EL devices were 2 × 2 mm². EL spectra of the devices were measured by a PR650 fluorescence spectrophotometer. Luminance–current density–voltage (*L–I–V*) curves were recorded with a Keithley 2400 instrument. All measurements were carried out at room temperature under ambient conditions.

Materials. Tetrahydrofuran (THF) for spectral study was distilled over sodium/benzophenone, and toluene was distilled over P₂O₅. Other solvents were used as commercial p.a. quality. 2,5-Dibromoterephthalic acid (**1**)¹⁰ and 2,7-bis(4,4,5,5-tetramethyl-1,3,2-dioxaborolan-2-yl)-9,9-dihexylfluorene¹¹ were prepared according to literature procedures. All other chemicals were purchased from Aldrich and Acros and used without any further purification.

Synthesis. 3,6-Dibromo-2,5-phenylenendi(carboxylic acid chloride) (2). 2,5-Dibromoterephthalic acid (3.5 g, 10.5 mmol) was treated with 16 mL of thionyl chloride (SOCl₂) (205 mmol) and refluxed for 10 h. The excess SOCl₂ was removed in a vacuum to give 3.71 g of **2** as a crystalline yellow solid (yield: 95%). ¹H NMR (CDCl₃, 500 MHz): δ 8.208(s, 2H).

2',5'-Dibromo-4-decyl-4'-(4-decylbenzoyl)benzophenone (3). To a solution of decylbenzene (7.2 mL, 28.4 mmol) and aluminum trichloride (2 g, 14.98 mmol) in 15 mL of benzene, a mixture of **2** (2.04 g, 5.67 mmol) and 5 mL of benzene was added dropwise. After stirring at room temperature for 48 h the mixture was poured into ice/2 M HCl. The organic layer was washed with 1 M NaOH and water, then dried over MgSO₄ and concentrated. The residue was recrystallized from acetone to give **3** of 2.89 g as a white crystal

(yield: 72.3%). ¹H NMR (CDCl₃, 500 MHz): δ 7.76 (d, 4H), 7.582 (s, 1H), 7.32 (d, 4H), 2.69 (t, 4H), 1.65 (t, 4H), 1.26 (m, 28H), 0.88 (t, 6H). Anal. Calcd: C, 66.30; H, 7.23; O, 4.42. Found: C, 66.47; H, 7.30; O, 4.45.

Polymer P1. A mixture of **3** (150.4 mg, 0.21 mmol), 2,7-bis(4,4,5,5-tetramethyl-1,3,2-dioxaborolan-2-yl)-9,9-dihexylfluorene (121.2 mg, 0.21 mmol), tetrakis(triphenylphosphino)palladium(0) (8 mg), 3 mL of toluene, and 1 mL of 1 M K₂CO₃ was refluxed for 48 h under nitrogen. The mixture was poured into water and extracted with dichloromethane. The organic layer was washed with brine and water, then dried over MgSO₄ and concentrated; the polymer was precipitated into methanol (1:10), and the crude product was dissolved in dichloromethane and reprecipitated into methanol (1:10) to give **P1** of 122.7 mg as a yellow-green solid (yield: 65%). ¹H NMR (CDCl₃, 500 MHz): δ 7.588–7.573 (d, 4H), 7.529 (s, 2H), 7.390–7.374 (t, 2H), 7.249–7.236 (m, 2H), 6.975–6.958 (s, 2H).

Polymer P2a. A solution of polymer **P1** (100 mg, 0.11 mmol) in 40 mL of toluene was treated with a solution of 1.6 M methyllithium in diethyl ether (1 mL, 1.6 mmol). The mixture was stirred 30 min at room temperature and carefully quenched with ethanol, water, and dilute hydrochloric acid. The organic layer was washed with water, dried with MgSO₄, and concentrated to dryness. The crude polymer was redissolved in tetrahydrofuran and precipitated into water to give 91 mg of colorless solid (yield: 87%).

Polymer P2b. A solution of polymer **P1** (100 mg) in 10 mL of toluene was added to a suspension of LiAlH₄ (40 mg) in 10 mL of THF. The mixture was stirred for 30 min at room temperature and carefully quenched with ethanol, water, and dilute hydrochloric acid. The organic layer was washed with water, dried, and concentrated. The polymer was redissolved in THF and precipitated in water to give 87 mg of colorless solid (yield: 84%).

MeLPF. A solution of polymer **P2a** (100 mg) in 20 mL of methylene chloride was treated with boron trifluoride etherate (300 mg, 2.11 mmol). After stirring for 5 min at room temperature, 10 mL of ethanol was added to the mixture to destroy the catalyst. The organic layer was then carefully washed with water, dried, and concentrated. Precipitation in methanol gives 89 mg of MeLPF as a yellow-green powder (yield: 87.8%). ¹H NMR (CDCl₃, 500 MHz): δ 7.57 (d, 4H), 7.38 (s, 2H), 7.21 (t, 4H), 7.09 (t, 4H), 2.56 (s, 4H), 1.95 (s, 4H), 1.25 (m, 32H), 1.07 (m, 12H), 0.88–0.53 (m, 16H). ¹³C NMR (CDCl₃, 100 MHz): δ 154.5, 154.1, 151.1, 141.3, 140.2, 128.7, 127.1, 115.6, 114.6, 54.2, 36.0, 32.3, 31.7, 30.2, 29.2, 26.4, 24.2, 23.1, 14.5. Anal. Calcd: C, 90.07; H, 9.93. Found: C, 88.54; H, 9.97.

HLPF. The procedure was the same as that of MeLPF. A yellow-green powder was obtained in 95.38% yield. ¹H NMR (CDCl₃, 500 MHz): δ 7.73 (s, 2H), 7.60 (s, 2H), 7.47 (s, 2H), 7.15 (t, 8H), 5.07 (s, 2H), 2.62 (s, 4H), 2.02 (s, 4H), 1.27 (m, 32H), 1.04 (m, 12H) 0.73–0.60 (m, 16H). ¹³C NMR (CDCl₃, 500 MHz): δ 155.4, 155.0, 151.4, 142.1, 141.0, 129.2, 129.0, 116.7, 115.0, 54.2, 36.2, 32.3, 31.9, 30.0, 29.7, 24.2, 23.1, 14.5. Anal. Calcd: C, 90.22; H, 9.78. Found: C, 89.33; H, 10.07.

Acknowledgment. This work is supported by National Natural Science foundation of China (Grant 20125421, 90101026, and 600777014) and by Ministry of Science and Technology of China (Grant 2002CB-6134003).

References and Notes

- (1) (a) Gustafsson, G.; Cao, Y.; Treacy, G. M.; Klavetter, F.; Colaneri, N.; Heeger, A. J. *Nature (London)* **1992**, 357, 477. (b) Kraft, A.; Grimsdale, A. C.; Holmes, A. B. *Angew. Chem., Int. Ed.* **1998**, 37, 402. (c) Friends, R. H.; Gymer, R. W.; Holmes, A. B.; Burroughes, J. H.; Marks, R. N.; Taliani, C.; Bradley, D. D. C.; dos Santos, D. A.; Bredas, J. L.; Lögglund, M.; Salaneck, W. R. *Nature (London)* **1999**, 397, 121.
- (2) (a) Grem, G.; Leising, G. *Synth. Met.* **1993**, 55–57, 4105. (b) Grüner, J.; Wttmann, H. F.; Hamer, P. J.; Friend, R. H.; Huber, J.; Scherf, U.; Müllen, K.; Moratti, S. C.; Holmes, A.

- B. *Synth. Met.* **1994**, 67, 181. (c) Tasch, S.; Niko, A.; Leising, G.; Scherf, U. *Appl. Phys. Lett.* **1996**, 68, 1090.
- (3) (a) Tasch, S.; Hochfilzer, C.; List, J. W. E.; Leising, G.; Quante, H.; Geerts, Y.; Schlichting, P.; Rohr, U.; Scherf, U.; Müllen, K. *Appl. Phys. Rev. B* **1997**, 56, 4479. (b) Yang, X. H.; Neher, D.; Scherf, U.; Bagnich, S. A.; Bäessler, H. *J. Appl. Phys.* **2003**, 93, 4413.
- (4) (a) Haugeneder, A.; Hilmer, M.; Kallinger, C.; Perner, M.; Spirk, W.; Lemmer, U.; Feldmann, J.; Scherf, U. *Appl. Phys. B: Laser Opt.* **1998**, 66, 389. (b) Schweitzer, B.; Wegmann, G.; Hertel, D.; Giessen, H.; Scherf, U.; Müllen, K.; Rühle, W. W.; Bäessler, H.; Mahrt, R. F. *Appl. Phys. Lett.* **1998**, 72, 2933. (c) Romanovskii, Y. V.; Gerhard, A.; Schweitzer, B.; Personov, R. I.; Bäessler, H. *Chem. Phys.* **1999**, 249, 29. (d) Lupton, J. M.; Pogantsch, A.; Piok, T.; List, J. W. E.; Patil, S.; Scherf, U. *Phys. Rev. Lett.* **2002**, 89, 167401.
- (5) Scherf, U.; Müllen, K. *Makromol. Chem., Rapid Commun.* **1991**, 12, 489.
- (6) (a) Lemmer, U.; Heun, S.; Mahrt, R. F.; Scherf, U.; Hopmeier, M.; Siegner, U.; Göbel, E. O.; Müllen, K.; Bäessler, H. *Chem. Phys. Lett.* **1995**, 240, 373. (b) Graupner, W.; Eder, S.; Tasch, S.; Leising, G.; Lanzani, G.; Nisoi, M.; de Silvestri, S.; Scherf, U. *J. Fluoresc.* **1995**, 7, 195s. (c) Mahrt, R. F.; Pauck, T.; Lemmer, U.; Siegner, U.; Hopmeier, M.; Hennig, R.; Bäessler, H.; Göbel, E. O.; Haring Bolivar, P.; Wegmann, G.; Kurz, H.; Scherf, U.; Müllen, K. *Phys. Rev.* **1996**, 54, 1759.
- (7) Scherf, U.; Bohnen, A.; Müllen, K. *Makromol. Chem.* **1992**, 193, 1127.
- (8) Scherf, U. *J. Mater. Chem.* **1999**, 9, 1853.
- (9) (a) List, E. J. W.; Guentner, R.; de Freitas Scanducci, P.; Scherf, U. *Adv. Mater.* **2002**, 14, 374. (b) Scherf, U.; List, E. J. W. *Adv. Mater.* **2002**, 14, 477. (c) Zojer, E.; Pogantsch, A.; Hennebicq, E.; Beljonne, D.; Brédas, J.; de Freitas Scanducci, P.; Scherf, U. *J. Chem. Phys.* **2002**, 117, 6794.
- (10) Forster, M. Novel Conjugated Polyarylene with Ladder Structure. Ph.D. Thesis, Johannes-Gutenberg-Universitaet Mainz, Germany (German), 2000; p 50.
- (11) (a) Ego, C.; Marsitzky, D.; Becker, S.; Zhang, J.; Grimsdale, A. C.; Müllen, K.; MacKenzie, J. D.; Silva, C.; Friend, R. H. *J. Am. Chem. Soc.* **2003**, 125, 437. (b) Oda, M.; Nothofer, H.-G.; Scherf, U.; Sunjic, V.; Richter, D.; Regenstein, W.; Neher, D. *Macromolecules* **2002**, 35, 6792. (c) Liu, B.; Yu, W.-L.; Lai, Y.-H.; Huang, W. *Macromolecules* **2002**, 35, 4975. (d) Setayesh, S.; Grimsdale, A. C.; Weil, T.; Enkelmann, V.; Müllen, K.; Meghdadi, F.; List, E. J. W.; Leising, G. *J. Am. Chem. Soc.* **2001**, 123, 946.
- (12) Yao, Y.; Tour, J. M. *Macromolecules* **1999**, 32, 2455.
- (13) Ranger, M.; Rondeau, D.; Leclerc, M. *Macromolecules* **1997**, 30, 7686.
- (14) Demas, J. N.; Crosby, G. A. *J. Phys. Chem.* **1971**, 75, 991.
- (15) Lupton, J. M. *Chem. Phys. Lett.* **2002**, 365, 366.
- (16) Haugeneder, A.; Lemmer, U.; Scherf, U. *Chem. Phys. Lett.* **2002**, 351, 354.

MA034929Q